

Runoff simulations using water and energy balance equations in the lower reaches of the Heihe River, northwest China

Zhuolun Li · Nai'ang Wang · Yu Li ·
Zhenyu Zhang · Mengna Li · Chunyu Dong ·
Rong Huang

Received: 18 October 2011 / Accepted: 29 October 2012
© Springer-Verlag Berlin Heidelberg 2012

Abstract Methods for reconstruction of river runoff have been an important component of paleo-climatology and paleo-hydrology. The lower Heihe River was studied from 2002 to 2008 to reconstruct the annual average runoff at the Zhengyi Gorges hydrological station using measured data and improved water and energy balance equations. The results indicate that the reconstructed annual runoff and the measured runoff values are not equivalent. However, the difference between reconstructed and measured runoff values is within 10 %, which suggests that water and energy balance models can successfully reconstruct runoff from rivers in arid regions. Regional differences imply that parameters must be corrected when applying water and energy balance equations to prevent large errors. In addition, the latent heat of evaporation in arid lakes is greater than their net radiation, according to latent and sensible heat calculations, which demonstrates the existence of the “cold island effect”.

Keywords Water balance equation · Energy balance equation · Runoff · Paleo-hydrology · Heihe River · Arid region

Introduction

Paleo-runoff contains abundant climate and hydrology information and is an important and difficult component of

paleo-climatology and paleo-hydrology research (Schumm 1965, 1977; Liu et al. 2010). Schumm (1965, 1977) applied established climatic–hydrologic variability relationships to estimate paleoclimatic conditions and the depth of the corresponding paleo-runoff, which was a significant breakthrough. This method forms the basis of research on paleo-runoff and has been applied elsewhere (Wang et al. 2004). Reconstruction of paleo-hydrology and paleo-runoff using tree-rings is also an efficient and widely used method (Pederson et al. 2001; Chalise et al. 2003; Polacek et al. 2006; Liu et al. 2010). Reconstruction of runoff using tree-rings has a relatively higher temporal resolution, but this technique is not suitable for reconstruction of paleo-runoff and paleo-hydrology at large time scales. Reconstruction of paleo-hydrologic conditions at large time scales or within a specific climate period can enrich research on paleo-hydrology and is crucial to understanding past environmental changes.

Water and energy balance equations have been applied to reconstructions of paleo-precipitation in drainage basins since the 1980s (Kutzbach 1980; Hastenrath and Kutzbach 1983, 1985; Swain et al. 1983; Winkler et al. 1986). These equations are important methods in paleo-climatology and paleo-hydrology research, especially in arid and semi-arid areas, which are sensitive to precipitation (Jia et al. 2004). Water levels in terminal lakes are affected by runoff precipitation, evaporation, and other factors. Therefore, water level changes in inland lakes are a result of the balance between precipitation, runoff, and evaporation (Shi et al. 2002; Li and Morrill 2010). In addition to indicating climate change (Shi 1990; Harrison 1993; Hu et al. 1994; Zhang et al. 2004), water level changes in lakes can reflect the volume of runoff to a degree, especially in extremely arid areas, where runoff has a more intensive effect on hydrology changes in terminal lakes. Previous research

Z. Li (✉) · N. Wang · Y. Li · Z. Zhang · M. Li · C. Dong ·
R. Huang
College of Earth and Environmental Sciences, Center for
Hydrologic Cycle and Climatic Change in Arid Region, Lanzhou
University, Lanzhou 730000, China
e-mail: lizhuolunzl@163.com

mainly applies the balance equations to reconstruct paleo-precipitation within a drainage basin (Kutzbach 1980; Wu et al. 1993; Guo et al. 2000; Jia et al. 2000, 2001a, b; Hu et al. 2003; Zhao et al. 2007; Rhode et al. 2010; Zhu et al. 2010). In recent years, improvements to the water and energy balance equations have resulted in predictions of water level changes in Qinghai Lake (Qu 1994; Dong et al. 2009) and reconstruction of paleo-runoff in a drainage basin (Qin 1997). However, the application of water and energy balance equations to reconstruct paleo-runoff and related aspects in a terminal lake, especially in areas with highly variable precipitation and runoff, require further study.

The Heihe River basin is the second largest inland river basin in China. The terminal lake area in its lower reaches, which mainly consists of desert and swamp, is located in the monsoon-westerlies transition zone, and the climate is extremely arid (Ma et al. 2011). The water supply of the terminal lake depends on the Heihe River (Ge et al. 2009); therefore, water and energy balance equations can be applied. However, these equations have rarely been used in this region. The application of improved water and energy balance equations can establish a new basis for research on environmental change and hydrologic cycles in this region. Moreover, the improved equations can serve as a new reference and paradigm for the application of water and energy balance equations.

Using measured meteorological and hydrologic data, this paper explores the feasibility of runoff calculations in a terminal lake area using improved water and energy balance equations. The accuracy of water and energy balance equations in this region is demonstrated in this study, and also provides a reference for the reconstruction of paleo-runoff and paleo-climate.

Study area

The Heihe River originates in the Qilian Mountains in Qinghai province, and flows through the Hexi Corridor of Gansu Province and enters the western part of the Inner Mongolian Plateau, roughly at geographical coordinates 98°–101°30'E, 38°–42°N (Fig. 1). The vegetation in the basin is shown in Fig. 2. The basin length is approximately 821 km, and the total area is $13 \times 10^4 \text{ km}^2$. The Heihe River is divided into the upper reaches, middle reaches, and lower reaches by the Lingluo Gorge and Zhengyi Gorge: above Yingluo Gorge is the upper reaches, between Yingluo Gorge and Zhengyi Gorge is the middle reaches, and below Zhengyi Gorge is the lower reaches, which is called the Ruoshui alluvial fan. The upper reaches are located in Gansu and Qinghai Provinces. The middle reaches are located in the Hexi Corridor, Gansu Province, and the lower reaches are located in the Ejin Banner and Jiuquan

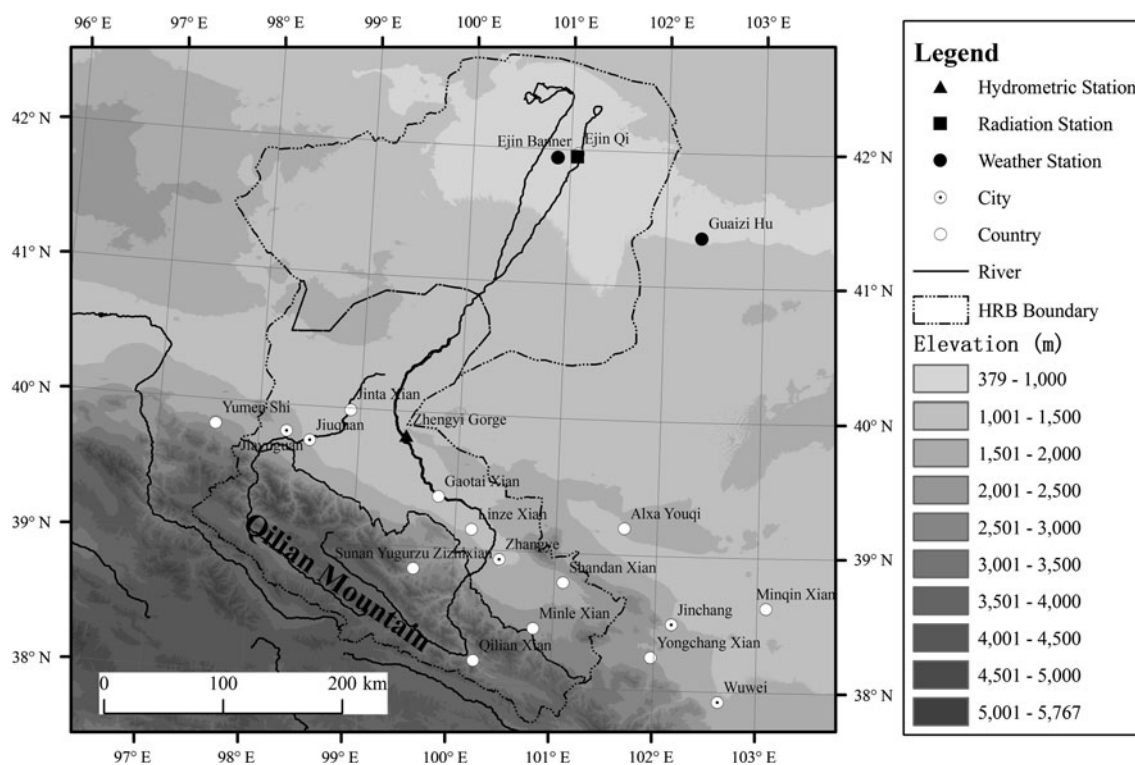


Fig. 1 Map of the research area showing the elevations (m) and the distribution of rivers around the Heihe River

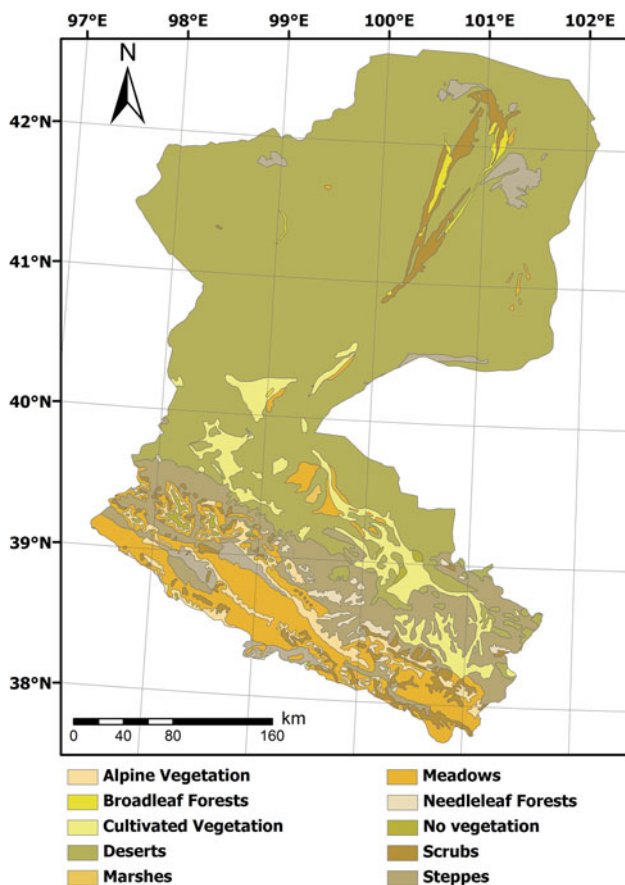


Fig. 2 The vegetative distribution map of the Heihe River Basin. The vegetation data is provided by “Environmental & Ecological Science Data Center for West China, National Natural Science Foundation of China” (<http://westdc.westgis.ac.cn>)

area. (1) The upper reaches are 303 km long, and the area is $1.71 \times 10^4 \text{ km}^2$, with an elevation of 3,000–5,000 m above sea level (ASL). The forest zone has an altitude of 3,000–4,000 m. Above 4,000 m is snow-covered annually, with glacier development at altitudes higher than 4,500 m. With increasing altitude in shady slopes, the vegetation zones can be categorized as mountainous desert, mountainous forest and alpine scrub. The climate is cold, with mean annual temperatures from -3 to $3 \text{ }^\circ\text{C}$, and annual precipitation is approximately 350–400 mm, most of which occurs in summer (Ding et al. 2009). The upper reaches are the primary areas for generation of runoff. (2) The middle reaches are 185 km long, and the area is $2.56 \times 10^4 \text{ km}^2$, with an elevation of 1,300–1,700 m decreasing from south to north. There are mountains of intermediate height and diluvial plain in this region. The mean annual temperature is $7 \text{ }^\circ\text{C}$, and the annual precipitation is 130 mm; however, evaporation is more than 1,200 mm (Lan et al. 2004). Therefore, the irrigated agricultural area in the middle reaches depends upon the Heihe River for water resources. The middle reaches are also the largest consumptive areas

in the entire river. The land types can be categorized as forest land, grassland, plow land, desert and Gobi (Li et al. 2009; Zhou et al. 2009). (3) The lower reaches have an elevation of 900–1,300 m, and the terrain is generally flat. The southwest and northern areas are mainly alluvial plain and aggraded flood area. The central basin consists primarily of alluvial and lake plain, and the northeastern area, bordering the Badain Jaran Desert, is an ancient alluvial plain. Most of the lower reaches region is desert or Gobi, and the climate is extremely arid. The average annual precipitation values for Ejin Banner and Guaizi Lake are only 35.5 and 42.9 mm, respectively (Ma et al. 2011), with an average annual temperature ranging from 8 to $10 \text{ }^\circ\text{C}$. This area is among the most arid in China, as well as one of the main source areas for dust storms in northern China (Wang et al. 2000; Gong et al. 2002; Guo et al. 2003; Li et al. 2004). Common vegetation in the Ejin basin delta includes *Populus euphratica*, *Eaeagnus angustifolia*, *Tamarix chinensis*, and *Glycyrrhiza uralensis*. In the meadows and shrubs near the river banks, the seeding of forests is closely related to river runoff, while desert forest and shrubby growth are maintained by underground water sources, which rely, to a greater extent, on the river runoff (Ge et al. 2009). In the Gobi area of the lower reaches, the radiation budget varies significantly with season. Generally, the daily total radiation in winter is less than half of that in summer, and the net radiation is slightly more than 25 % of that in summer. However, the annual total radiation is high ($>6,500 \text{ MJ m}^{-2}$; Wang et al. 2009).

The mountains are the place where runoff generates and water resources form, and the basins are the place where water resources disappear (Wu et al. 2004). The upstream region in the mountains is the flow accumulation zone, the middle alluvial plain region is the primary zone of human water usage, and the downstream desert area is where runoff disappears through evaporation and infiltration (Zhu et al. 2004). In the runoff usage zone of the arid inland river basins, the surface water–groundwater–surface water cycle often repeats two to three times. The main water cycle processes are as follows:

The runoff of the river from the mountain areas consists of ice-snow melted water, precipitation, and the groundwater in the mountains (Lan et al. 2004; Wu et al. 2010a; Li et al. 2012b). Among them, precipitation is the main supply (Li et al. 2012b), and the fluctuations of it often cause corresponding runoff fluctuations in the upper reaches of the Heihe River Basin. The monthly mean runoff and the monthly precipitation in the Heihe River mountainous watershed has perfect linear relationship (Chen et al. 2002). About 70–80 % of the annual precipitation is concentrated in the months from June to September, while less than 5 % occurs in the winter months from December to February (Chen and Qu 1992; Li et al.

1999). Hence, most of the upper stream inflow occurs in the flood season (Li and Liu 2004; Lan et al. 2005; Zhang et al. 2007). According to the Glacier Inventory of China (Wang et al. 1981), there are 1,078 glaciers covering 420.55 km² in the Qilian Mountains of the Heihe River Basin. The alimentary ratio of the glacial melt water to the total river runoff is 8 % on average (Yang 1991). Once the runoff comes from melted water and precipitation in the mountains enters the basins, frequent transformation between surface water and groundwater takes place (Wu et al. 2004). The local hydrological cycle starts with surface water going underground at the foot of the mountains, then re-emerging at the lower portion of the plain to form surface water again. During the runoff out of the mountains, large amounts of water infiltrate into underground and change to groundwater (Wu et al. 2004; Nie et al. 2005). Under the alluvial plain, there is abundant groundwater storage in the thick, porous Quaternary strata. Groundwater is replenished by infiltration from rivers and from subsurface flow (Feng et al. 2004; Wu et al. 2004; Cheng et al. 2010). Some of the loss in groundwater can be attributed to spring (surface) outflow on alluvial fan front (Feng et al. 2004). The runoff and groundwater completed the cyclic transformation mutually for the first time (Feng et al. 2004; Wu et al. 2004; Cheng et al. 2010).

In middle reaches (Zhangye–Linze–Gaotai Basin), surface water is converted to shallow groundwater by lateral inflow and irrigation (Qin et al. 2011), and then shallow groundwater loses in vertical surface evaporation and vegetation transpiration (Qin et al. 2011; Li et al. 2012a). In lower reaches (Ejin Banner basin), there are three connected groundwater systems after groundwater is recharged by the runoff: the deep, middle, and shallow groundwater flow systems (Zhu et al. 2004). Analytical results of environmental tracers and groundwater level show that the deep groundwater flow system recharges the middle groundwater flow system and the shallow groundwater flow system, and most shallow groundwater loses in vertical surface evaporation and desert vegetation transpiration (Zhu et al. 2004; Su et al. 2007; Cheng et al. 2010; Qin et al. 2011; Li et al. 2012a), small amount of shallow groundwater flows into the terminal lake. The water completed the cyclic transformation mutually for the second time.

In addition, the average annual precipitation is less than 100 mm in the lower reaches (Ma et al. 2011), whereas the average annual potential evaporation is more than 1,000 mm (Jia et al. 2009), which is far higher than precipitation. At the same time, rainfall events of 5 mm or less comprised 82 % of the rainfall events in the Heihe River basin (Zhang and Zhao 2008). Precipitation of more than 5 mm which is defined as the effective precipitation in arid desert could supply groundwater directly when the depth of the water tables is less than 1 m (Wu et al. 2010b).

However, the depth of the water tables is almost more than 3 m in the lower reaches area (Wu et al. 2010b). Therefore, it is difficult for the precipitation to supply groundwater directly in the lower reaches area. Compared to the local precipitation, surface water is the main source that contributes to the groundwater supply (Qin et al. 2011). The water consumption of desert vegetation equals to a cumulative effective precipitation (Zhao and Liu 2010; Zhao et al. 2010), and groundwater which has been stored is consumed by the oasis (Cheng et al. 2010).

Hence, the study water area (from the lower reaches to the terminal lake) can be considered as a closed basin and the river flows into the terminal lake after recharging some of the groundwater. At the same time, groundwater is lost in vertical surface evaporation and desert vegetation transpiration. The lost groundwater is mainly supplied by the runoff of upper and middle reaches. However, surface hydrologic processes have little impact on underground processes in desert riparian forest in the lower reaches of the Heihe River (Cheng et al. 2010).

Data and methods

Data

The data used in this paper mainly consist of meteorological, hydrological, radiation, and remote sensing images. Spatial and temporal resolutions of these data are provided in Table 1.

The design of water and energy balance equations

Cheng et al. (2010) found that surface hydrologic processes had little impact on underground processes in desert riparian forest in the lower reaches of the Heihe River, which suggested that groundwater was consumed by the forest rather than converted from surface water and stored. In other words, the amount of supplemental water was less than water consumption by vegetation in the oasis. Therefore, water discharge fluctuations from the Zhengyi Gorge could not cause corresponding groundwater level fluctuations in an oasis in the lower reaches of the Heihe River Basin (Cheng et al. 2010). Groundwater can thus be ignored when the water balance model is used. Instead, water from the Zhengyi Gorge hydrological station to the terminal lake was the focus because the terminal lake was dry from 1994 to 2001; water outputs consist of evaporation and infiltration, and inputs consist of precipitation and runoff. Ignoring human activities, the research objective conforms to the following water balance equation:

$$P + R - E - I = \Delta H \quad (1)$$

where P and R represent precipitation and runoff, respectively; E and I are evaporation and infiltration,

Table 1 The content of data for the research

Data type	Data content	Sequence length/year	Temporal/spatial resolution	Situation
Meteorological data	Temperature, water vapor pressure, cloud fraction	1993–2009	Month	Ejin weather station
	Evaporation and precipitation	1993–2009	Month	Ejin and Guaizi Lake weather stations
Hydrological data	Runoff	1993–2009	Year	Zhengyi Gorge Hydrological station
Radiation data	Monthly total amount of radiation, net radiation, scatter radiation, and reflective radiation	1993–2009	Month	Radiation station of Ejin
Remote sensing data	TM and ETM+	2000–2009	30 m	East and west Juyan Lake
	HR	Sep. 2008	2.36 m	From Zhengyi Gorge to the terminal lake

respectively; and ΔH is the magnitude of lake-level fluctuations. Assuming that the lake surface is relatively constant, the water balance model can be expressed as:

$$P + R = E + I \tag{2}$$

The formula suggests that the amount of precipitation plus runoff is equal to the sum of evaporation and infiltration. The formula above can be expanded into:

$$P_w S_w + R = E_w S_w + I \tag{3}$$

where P_w is precipitation at the water surface; S_w is the area of the water surface; R is the runoff; E_w is the evaporation at the water surface and I is the infiltration amount of the river channel and lake. The water surface area can be divided into the river channel area (S_{w1}) and lake surface area (S_{w2}); therefore, the modified form of water balance model is:

$$P_w S_{w1} + P_w S_{w2} + R = E_w S_{w1} + E_w S_{w2} + I \tag{4}$$

Here, S_{w1} and S_{w2} can be calculated roughly using remote sensing images. P_w is the measured precipitation data at the Ejin and Guaizi Lake weather stations in the Heihe River lower reaches, and R uses Zhengyi Gorge data. E_w can be evaluated using pan evaporation (large area of a pan), and other data can be observed at weather stations. However, if the equations are used to reconstruct paleo-runoff, water surface evaporation can be acquired by calculating the latent evaporation using the energy balance formula (Kutzbach 1980):

$$E = \frac{R'}{(1 + B)L} \tag{5}$$

where R' is the net radiation (W/m^2), B is the Bowen ratio, and L is the latent evaporation, which varies with temperature. However, L is considered to equal $0.0769 W/m^2$ when the temperature ranges from 0 to 30 °C (Dong et al. 2009). Net radiation can be calculated using the formula:

$$R' = G_0(1 - \alpha)(1 - C) - A\epsilon\delta T^4 \tag{6}$$

where G_0 is the clear-sky solar total radiation (W/m^2), α is the surface reflectivity, C is the cloud fraction, A is the Angstrom coefficient, ϵ is the surface emissivity which is considered to 0.96 (Sellers 1965; Hastenrath and Kutzbach 1983, 1985), δ is the Stefan–Boltzman constant ($5.67 \times 10^{-8} \frac{W}{m^2 K^4}$), and T is air temperature (K). The formula for calculating the Angstrom coefficient is:

$$A = (a_1 - b_1\sqrt{e})(1 - c'C^2) \tag{7}$$

where c' is the Berliand latitude coefficient, e is the water vapor pressure (mb), and C is the cloud-sky cover ratio. a_1 and b_1 are coefficients determined from a global database (Berliand and Berliand 1952).

The runoff (R) can be calculated using Eqs. (4)–(7).

Results and discussion

From Eqs. (4)–(7), reconstruction precision was affected by evaporation, precipitation, water area and infiltration. After adjustment of parameters, these factors were simulated and runoff could be reconstructed. Moreover, Eqs. (5) and (6) showed that evaporation was influenced by long-wave radiation and the Bowen ratio. Therefore, to improve the precision of evaporation estimates, long-wave radiation, and Bowen ratios must be verified.

The Angstrom coefficient and net long-wave radiation

Previous research has established that the definitions of parameters in Eq. (7) influence the calculation results. However, the evaluation of this issue varies from investigator to investigator. The definitions of a_1 and b_1 are consistently 0.39 and 0.058, respectively, in almost all studies (e.g., Bergonzini et al. 1997; Jia et al. 2000, 2001b; Shen et al. 2005). The Berliand coefficient depends on the

latitude. In the Huahai region, Hexi Corridor, c' was 0.53 (Hu et al. 2003); in the Tibetan Plateau, c' was 0.65 (Qin 1994; Jia et al. 2000, 2001a, b) and 0.56 (Kou et al. 1981); in the Shiyang River Basin, c' was 0.62 (Zhao et al. 2007). The terminal lake of the Heihe River is located between 41° and 43°N latitude, and c' should range from 0.68 to 0.70 (Budyko 1974). Although a_1 and b_1 in the Angstrom coefficient equation are defined consistently by researchers, a_1 and b_1 are determined by Berliand and Berliand (1952) through a global database. Moreover, the results suggest that this equation can be applied effectively when the humidity is intermediate or high, but large errors may occur when the humidity is relatively low (Efimova 1961). In areas with low humidity, the following equation was suggested by Efimova (1961):

$$A = (0.254 - 0.0066e)(1 - c'C^2) \tag{8}$$

In the equation, the variables are the same as those in Eq. (7), but the selection of Eq. (7) or (8) mostly depends on the relative humidity. For example, Eq. (7) was applied for the Lake Tanganyika region (Africa) because the climate is tropical grassland (Bergonzini et al. 1997). In China, the Angstrom coefficient has been calculated using Eq. (7) in the Tibetan Plateau region (Jia et al. 2000, 2001a, b) and in the northwest arid region (Hu et al. 2003; Zhao et al. 2007). However, application of Eq. (7) in the northwest arid area of China requires verification. Evaluation and verification of the parameters used to calculate the Angstrom coefficient, along with selection of the appropriate equation based on humidity, are important steps for calculating the net long-wave radiation.

Monthly data from the weather and radiation stations in Ejin were evaluated during the period from January 1993 to December 2009. The radiation data include total monthly radiation (G_1), total monthly reflected radiation (G_2) and total monthly net radiation (R'). The meteorological data include water vapour pressure (e), cloudiness (C) and temperature (T), and annual averages were calculated from these monthly data. The relationship between G_1 , G_2 and R' can be expressed as:

$$G_1 - G_2 = G_3, \tag{9}$$

where G_1 is the total radiation, G_2 is the reflected radiation, and G_3 is the net short-wave radiation. The total monthly net radiation (R') and G_3 have the following relationship:

$$R' = G_3 + G_4, \tag{10}$$

where G_4 is the net long-wave radiation, which is calculated as:

$$G_4 = -A\varepsilon\delta T^4. \tag{11}$$

The variables in Eq. (11) are the same as those in Eq. (6). Different values for the underlying surface have a slight influence on ε (surface emissivity), and ε can be defined as 0.95 (Budyko 1974). The calculation of A can be completed with Eqs. (7), (8) and (11). Equation (7) can thus be modified to:

$$A = -\frac{G_4}{\varepsilon\delta T^4} = \frac{G_1 - G_2 - R'}{\varepsilon\delta T^4}, \tag{12}$$

where all variables are equal to those in Eqs. (9)–(11). The results of the three equations are presented in Table 2.

Table 2 The calculation result of the Angstrom coefficient of Ejin from 1993 to 2009

	Years	$G_1 - G_2 - R'/(W/m^2)$	$\varepsilon\delta T^4$	A ^a	A ^b	A ^c	A ^d	A ^e
	1993	116.564	339.960	0.343	0.238	0.238	0.200	0.199
	1994	121.746	344.201	0.354	0.243	0.242	0.204	0.204
	1995	117.968	341.817	0.345	0.246	0.245	0.207	0.207
	1996	124.230	340.805	0.365	0.243	0.242	0.204	0.204
	1997	123.990	345.342	0.359	0.248	0.248	0.209	0.208
	1998	118.750	349.181	0.340	0.233	0.232	0.197	0.197
	1999	115.615	347.118	0.333	0.239	0.238	0.202	0.202
	2000	116.605	343.943	0.339	0.245	0.244	0.205	0.205
^a Calculation result of Eq. (12)	2001	130.804	345.894	0.378	0.245	0.245	0.206	0.206
^b Calculation result of Eq. (7), and the values of a_1 , b_1 and c' are 0.39, 0.058 and 0.68, respectively	2002	120.414	347.265	0.347	0.237	0.237	0.200	0.200
	2003	122.285	342.825	0.357	0.231	0.231	0.196	0.196
	2004	129.706	346.075	0.375	0.238	0.238	0.200	0.200
^c Valuation of c' is 0.69, and the other parameters are the same as those in ^b	2005	114.338	344.611	0.332	0.243	0.243	0.203	0.202
	2006	117.650	346.075	0.340	0.237	0.237	0.199	0.198
	2007	130.782	347.584	0.376	0.234	0.233	0.198	0.197
^d Calculation result of Eq. (8), and c' is equal to 0.68	2008	123.178	345.665	0.356	0.245	0.244	0.205	0.205
^e c' is 0.69, and the remaining is the same as that in ^d	2009	121.174	337.718	0.359	0.247	0.246	0.204	0.204
	Average	121.518	344.475	0.353	0.241	0.240	0.202	0.202

The results from Eqs. (7) and (8) vary significantly from the actual value; however, results from Eq. (7) are closer to the actual values. If a_1 and b_1 are defined as 0.39 and 0.058, respectively, then net radiation will be higher, which is consistent with Efimova (1961). The effect of using different values for the Berliand coefficient was insignificant; therefore, the Berliand coefficient was defined as 0.68 in this paper.

The mean Angstrom coefficient was calculated from Eq. (12) for every 5-year period from 1993 through 2003. Water vapour pressure and the cloud-sky cover ratio (in tenths) were also determined for this period. Using the equations, the ultimate values of a_1 and b_1 were 0.535 and 0.07, respectively. Equation (7) can thus be modified to:

$$A = (0.535 - 0.07\sqrt{e})(1 - 0.68C^2), \tag{13}$$

where the parameters are the same as those in Eq. (8). The annual Angstrom coefficient from 1993 to 2009 was calculated using Eq. (13). The means for these calculations were similar (Fig. 3). The results from Eq. (13) are less than those from Eq. (12) by 0.011, which is an acceptable difference. The Angstrom coefficient results from Eqs. (12) and (13) were used to calculate G_4 using Eq. (11). The annual net long-wave radiation (G_4) was also calculated using Eqs. (9) and (10), and the means of the different calculations were nearly equivalent despite some differences in the results. The results from Eq. (11) were lower than those from Eq. (10) by 1.2 %, which is sufficiently accurate for these calculations.

The Bowen ratio

The Bowen ratio of the water surface (B) is calculated from Eq. (5). The amount of water surface latent evaporation (E)

was measured annually at both Ejina and Guaizi Lake, and total net radiation (R') was calculated using the radiation data from these stations. The detailed calculations are described below.

The water surface net long-wave radiation (G_4) can be estimated using Eqs. (11) and (13). The water vapour pressure at the lake surface (e) cannot be obtained by observation, and e was defined as 2 hPa above the water vapour pressure observed for land (Yu et al. 2001). The temperature at the lake surface is higher than that of the land by 2 °C.

The net short-wave radiation can be calculated as:

$$G_3 = G_1 \times (1 - \alpha) \tag{14}$$

where G_3 is the water net short-wave radiation, G_1 is the total radiation, and α is the water reflectivity, which was defined ($\alpha = 0.08$) based on observations of annual mean reflectivity at 40°N latitude (Budyko 1974). The results are presented in Table 3.

The water surface Bowen ratio calculated here does not agree with those from southeast Inner Mongolia (Shen et al. 2005), the Tibetan Plateau (Jia et al. 2001a, b) or the eastern Hexi Corridor (Zhao et al. 2007). According to Kutzbach (1980) and Priestley and Taylor (1972), the Bowen ratios of lake surfaces are between 0.1 and 0.2, and the Bowen ratios of the Tibetan Plateau and southeast Inner Mongolia are approximately 0.2. However, the Bowen ratio was approximately -0.5 in the present study. The differences can be attributed to the extremely arid climate of the region, which has a ground surface comprised mainly of Gobi and desert (Chen 2010), with an annual precipitation of approximately 40 mm (Ma et al. 2011). Due to asymmetrical heat from solar radiation in varied underlying surfaces, an oasis or lake in an arid area, such as

Fig. 3 The variability of the Angstrom coefficients acquired using different equations from 1993 to 2009. (1) is the calculation result from Eq. (12), (2) is the result from Eq. (13), (3) is the net long-wave radiation from Eq. (10), and (4) is the absolute value of the net long-wave radiation from Eq. (11)

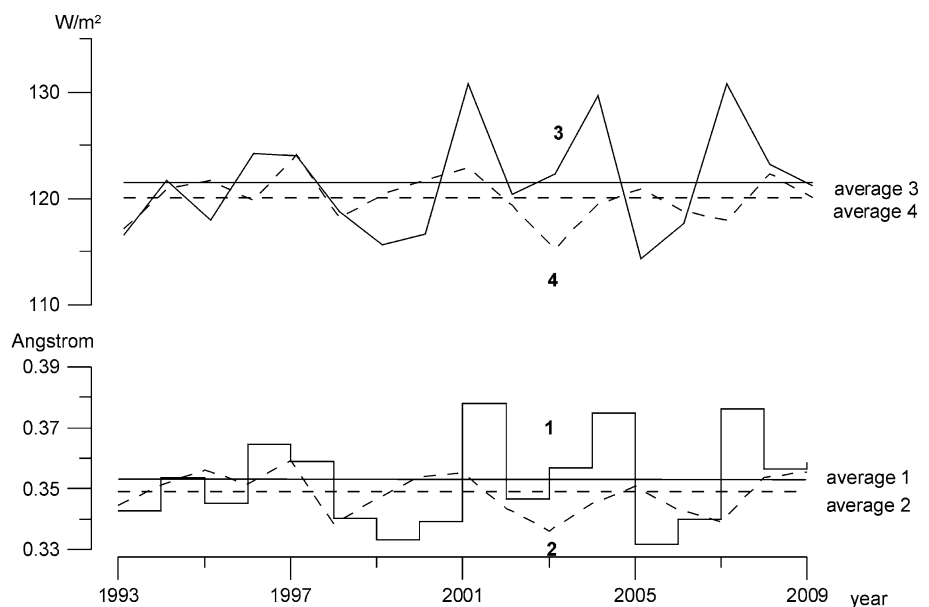


Table 3 The calculation results of the water surface Bowen ratio

Years	Annual evaporation amount (mm)	The net short-wave radiation of the water (G_3)	The net long-wave radiation of the water surface (G_4)	The total net radiation of the water surface (R')	The Bowen ratio of the water surface (B)
1993	2,189.685	192.644	-111.108	81.536	-0.518
1994	2,184.787	192.671	-114.731	77.940	-0.558
1995	2,198.613	193.718	-115.537	78.181	-0.539
1996	2,295.395	192.381	-113.669	78.713	-0.537
1997	2,206.27	195.676	-117.740	77.937	-0.567
1998	2,211.881	183.601	-112.264	71.337	-0.613
1999	2,338.578	184.742	-114.383	70.358	-0.605
2000	2,395.587	190.560	-115.536	75.024	-0.579
2001	2,313.716	194.697	-116.552	78.146	-0.593
2002	2,315.762	190.503	-113.301	77.202	-0.571
2003	2,494.384	187.804	-109.585	78.219	-0.530
2004	2,342.087	192.178	-113.319	78.859	-0.589
2005	2,164.179	191.301	-114.551	76.751	-0.595
2006	2,495.538	185.433	-112.642	72.791	-0.619
2007	2,461.616	181.686	-112.026	69.660	-0.632
2008	2,486.736	188.021	-115.952	72.069	-0.625
2009	2,460.32	194.373	-113.609	80.763	-0.581
Average	2,345.194	190.117	-113.912	76.205	-0.579

desert and Gobi, may become a cold source relative to the surrounding environment. This phenomenon may result in a cold island effect, which is the opposite of the heat island effect (Su and Hu 1987). The cold island effect is an inevitable consequence of the heterogeneity of underlying surfaces (Zuo et al. 2004). For the oasis and desert areas of the Heihe River, Wang et al. (2009) concluded that energy transfer to the atmosphere as latent heat was much higher than that in the Gobi and desert areas. Energy transferred by Gobi and desert areas was mainly as sensitive heat, with less influence from latent heat. This pattern suggests a heat advection transfer from the desert and Gobi areas to the oasis, thus resulting in the cold island effect.

Evaporation calculation

Average annual data (1993–2009) from the weather and radiation stations in Ejina and Guaizi Lake were evaluated. From Eqs. (5)–(7), evaporation calculation results in different parameters and pan evaporation (large area of a pan) observed data are shown in Table 4. By contrast, the equations which parameters have been corrected for the modern water area in the lower reaches of the Heihe River are consistent between observed and calculated evaporation. It shows that the equations have high accuracy in calculating the evaporation.

Table 4 Evaporation calculation results in different parameters and pan evaporation observed data (large area of a pan, 1993–2009 average)

Calculative process	Observed data	(a)	(b)	(c)	(d)
Evaporation/mm	2,345	1,317	870	3,603	2,378

From Eqs. (5)–(7) [(a) B is 0.15, a_1 is 0.39 and b_1 is 0.058; (b) B is 0.15, a_1 is 0.535 and b_1 is 0.07; (c) B is -0.579, a_1 is 0.39 and b_1 is 0.058; and (d) this paper, B is -0.579, a_1 is 0.535 and b_1 is 0.07]

Some parameters in the equations should be corrected using modern meteorological data. Previous research may over-estimate net radiation and the Bowen ratio in arid regions of China (e.g., Jia et al. 2000, 2001a, b; Hu et al. 2003; Zhao et al. 2007). From this study, previous definitions of parameters in the equations were not suitable for arid regions in China, which would cause lower Angstrom coefficient values (Table 2). Calculated values of net long-wave radiation thus were lower, while net radiation was higher. In addition, previous research has shown that lake surface Bowen ratios were between 0.1 and 0.2 in Africa (Kutzbach 1980; Priestley and Taylor 1972), which was due to tropical study areas. However, in arid Central Asia, cold island effects caused the Bowen ratio to be lower than in tropical zones. Consequently, evaporation calculated from the water and energy balance equations will vary significantly without correcting the parameters (Table 4).

Calculation of infiltration

Infiltration of channel and lake-faces is difficult to measure. The middle reaches of the Heihe River are responsible for 83 % of the total water dissipation in the area (Qian and Wang 2008). Evaporation and infiltration account for most of the water dissipation in the lower reaches, and artificial water consumption accounts for 15 % of the runoff (Qian and Wang 2008). To simplify the calculation, it can be assumed that the area of the channel is constant when the lake is dry throughout the year. Precipitation can also be ignored in this arid region. Thus, Eq. (4) can be modified to:

$$I = R(1 - a) - E_w S_{w1}, \tag{15}$$

where *a* is the water utilization rate (15 %), and the remaining variables are the same as those in Eq. (4). The results from Eq. (15) from 1995 to 2001 are presented Table 5. The evaporation data are the same as in Table 3, and the channel area is estimated based on high resolution (HR) image data.

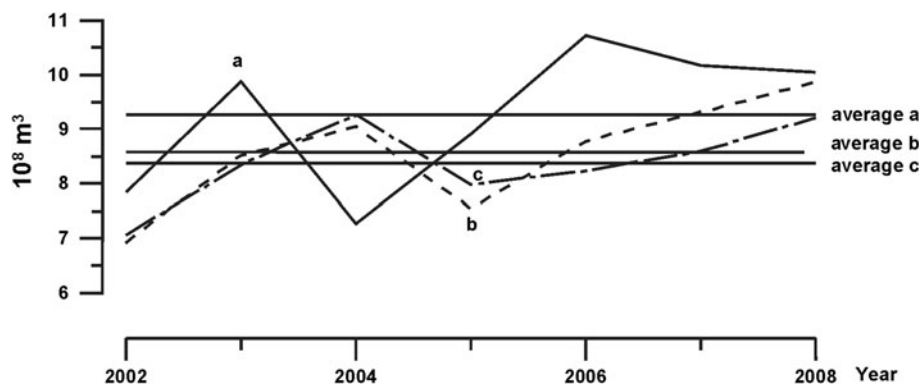
Reconstruction of the runoff

Using Eqs. (4)–(7) and (15), the yearly runoff for the Zhengyi Gorge from 2002 to 2008 was calculated. In these

Table 5 The river channel infiltration amount in the Hei River terminal lake area from 1995 to 2001

Years	Runoff/ 10 ⁸ m ³	Evaporation amount/ 10 ⁸ m ³	Infiltration amount/ 10 ⁸ m ³
1995	7.05	3.748	2.245
1996	9.52	3.913	4.179
1997	5.14	3.761	0.608
1998	11.22	3.770	5.767
1999	7	3.986	1.964
2000	6.591	4.084	1.519
2001	6.48	3.944	1.564
Average	7.571	3.887	2.549

Fig. 4 The variability of reconstructed annual runoff of the Zhengyi Gorge using different parameters [a the measured annual runoff; b the calculation result from Eq. (15); and c the calculation result from Eqs. (4)–(7)]



calculations, the yearly lake surface area was determined seasonally from the average rough calculations based on image data from TM and ETM+. At the same time, the Bowen ratio of the water surface was defined as -0.58 , and the Angstrom coefficient of the water was defined as 0.353 . R' was calculated with the values from Table 3, and the channel infiltration was the average value ($2.549 \times 10^8 \text{ m}^3$, Table 5).

The reconstructed results (Fig. 4) indicate that the annual runoff calculated from the improved water balance Eq. (15) is similar to those from Eqs. (4)–(7).

Both of the reconstructed results have discrepancies with the measured annual runoff data. Assuming that the lake levels were stable when the equations were used, the lake area was averaged seasonally. Both infiltration in the channel and the Bowen ratio were also averaged values. Hence, there are errors between the annual reconstructed result and actual data, but the accuracy of the average runoff from 2002 to 2008 was higher than the annual runoff variability, and the difference between the reconstructed and measured results was $<10\%$. Therefore, this method can be applied successfully to reconstruct changes in paleo-runoff in defined time periods.

The applicability of water and energy balance equations

Water and energy balance equations have been applied in tropical lakes to estimate increases in paleo-precipitation at 9 ka BP in Africa (Kutzbach 1980). The equations were used subsequently for basin precipitation reconstruction (Kutzbach 1980; Wu et al. 1993; Guo et al. 2000; Jia et al. 2000, 2001a, b; Zhao et al. 2007; Rhode et al. 2010; Zhu et al. 2010). Qin (1997) estimated Qinghai Lake Basin precipitation and runoff during the mid-Holocene period on the Qinghai–Tibet Plateau, and modern precipitation was also estimated, with verifications from current meteorological data. Bergonzini et al. (1997) inferred the mean and range of annual evaporation and precipitation in the Tanganyika basin during the LGM, and the equations used for the modern basin were consistent between observed and

simulated hydrological variables. These studies show that reconstructed precipitation is accurate and reliable when using water and energy balance equations. This study shows that the improved water and energy balance equations also can be applied in arid regions for basin precipitation and runoff reconstructions.

Lake area variability influenced total evaporation using the equations for paleo-runoff reconstruction in a closed basin, which influenced the runoff reconstructions. When the lake surface was stable over long time periods, or some geomorphological evidence (e.g., lake shorelines and terraces) indicated the lake attitude (Zhang et al. 2004; Wang et al. 2011), the areas and levels of these paleo-lakes could be reconstructed accurately. Thus, paleo-runoff could be reconstructed quantitatively or semi-quantitatively. When the lake had a large surface area during a specific period, such as the terminal lake of the Heihe River (>7,000 km² in MIS 3a; Wang et al. 2011), changes in the area of the river channel could be disregarded relative to waters in the lower reaches. The paleo river channel area can then be replaced by the present value. Moreover, as a long time scale, especially the lake surface relatively stable in a long time, because of inland terminal lake having a closed catchment basin, water infiltration would not need to be considered based on the fundamentals of water and energy models (Kutzbach 1980; Hastenrath and Kutzbach 1983). Paleo-precipitation could be reconstructed using proxy climate data and some previous researches to improve the accuracy of paleo-runoff estimates.

When the lake surface is relatively stable for long time periods, runoff into the inland terminal lake could be reconstructed with high accuracy and reliability. Thus, there are some advantages to reconstructing paleo-runoff during the late Quaternary period using this method. However, in interannual and decadal time scales, accurate water-level fluctuations could not be acquired, the paleo-runoff reconstructed was restricted. Other methods, such as tree-rings (e.g., Liu et al. 2010; Qin et al. 2010), emphasize paleo-runoff during the reconstruction period. For example, based on tree-ring-width analysis, the average runoff from the previous September to the subsequent June was reconstructed for the middle section of the Heihe River from 1430 to 2007 (Liu et al. 2010). In comparison, the superiority of runoff reconstruction using tree-rings over short time scales, especially at interannual and decadal time scales, is obvious; however, for time scales of 10³–10⁴ years, water and balance equations are suitable for reconstruction of paleo-runoff.

Conclusions

1. The improved water and energy balance equations can be applied to reconstruct the runoff in arid areas. The

accuracy of the reconstructed average runoff over several years was higher than that of the annual runoff. Consequently, this method can theoretically be used to reconstruct paleo-runoff in a specific period.

2. However, using the improved water and energy balance equations, the parameters must be corrected due to differences between regions. The different values for the parameters can cause large variability in the calculated results.
3. In arid areas, the amount of latent heat of evaporation is larger than that of the water net radiation, which demonstrates the existence of the cold island effect.

Acknowledgments I would like to express my sincere gratitude to the editor and anonymous reviewers who have put considerable time and effort into their comments on this paper. This study was supported by the National Natural Science Foundation of China (No. 50879033 and 41001116), Specialized Research Fund for the Doctoral Program of Higher Education (SRFD, No. 20090211110025), Fund for New Doctoral Candidate Academic in the Ministry of Education and the Fundamental Research Funds for the Central Universities (lzujbky-2010-221 and lzujbky-2012-222).

References

- Bergonzini L, Chalié F, Gasse F (1997) Paleoevaporation and paleoprecipitation in the Tanganyika Basin at 18,000 Years B.P. Inferred from hydrologic and vegetation proxies. *Quat Res* 47:295–305
- Berliand ME, Berliand TG (1952) Determining the net long-wave radiation of the Earth with consideration of the effect of cloudiness. *Izv. Akad. Nauk SSSR Ser. Geofiz. No. 1*
- Budyko MI (1974) Climate and life. In: *International Geophysics Series*, vol 18. Academic Press, New York, pp 58–59
- Chalise SR, Kansakar SR, Rees G, Croker K, Zaidman M (2003) Management of water resources and low flow estimation for the Himalayan basins of Nepal. *J Hydrol* 282:25–35
- Chen X (2010) Chinese physical geography in arid region. Science Press, Beijing, pp 286–287 (in Chinese)
- Chen L, Qu Y (1992) Water and land resources and their rational development and utilization in the Hexi Region. Science Press, Beijing, pp 3–9 (in Chinese)
- Chen RS, Kang ES, Yang JP, Zhang JS (2002) Nonlinear features of the runoff from mountain areas of the Heihe River, Qilian Mountains. *J Glaciol Geocryol* 24:292–298 (in Chinese with English abstract)
- Cheng GD, Xiao HL, Chen YN (2010) Ecology-hydrology research in typical continental river, west China. Science Press, Beijing, pp 206–207 (in Chinese)
- Ding R, Wang FC, Wang J, Liang JN (2009) Analysis on spatial-temporal characteristics of precipitation in Heihe River Basin and forecast evaluation in recent 47 years. *J Desert Res* 29:335–341 (in Chinese with English abstract)
- Dong CY, Wang NA, Li ZL, Yang P (2009) Forecast of lake level in Lake Qinghai based on energy-water balance model. *J Lake Sci* 21:587–593 (in Chinese with English abstract)
- Efimova NA (1961) On methods of calculating monthly values of net long-wave radiation. *Meteorol Gidrol* 10:28–33
- Feng Q, Liu W, Su YH, Zhang YW, Si JH (2004) Distribution and evolution of water chemistry in Heihe River basin. *Environ Geol* 45:947–956

- Ge XG, Xue B, Wan L, Hu FS (2009) Modelling of lagging response of NDVI in Ejina Oasis to runoff in the lower reaches of Heihe River. *Sci Geographica Sinica* 29:900–904 (in Chinese with English abstract)
- Gong JD, Cheng GD, Zhang XY, Xiao HL, Li XY (2002) Environmental changes of Ejina Region in the lower reaches of Heihe River. *Adv Earth Sci* 17:491–496 (in Chinese with English abstract)
- Guo XY, Chen FH, Shi Q (2000) The application of GIS and water and energy budget to the study on the water rebuilding of Paleolake—a case in Shiyang River drainage. *Scientia Geographica Sinica* 20:422–426 (in Chinese with English abstract)
- Guo N, Zhang J, Liang Y (2003) Climate change indicated by the recent change of inland lakes in northwest China. *J Gliciol Geocryol* 25:211–214 (in Chinese with English abstract)
- Harrison SP (1993) Late Quaternary lake-level changes and climates of Australia. *Quat Sci Rev* 12:211–232
- Hastenrath S, Kutzbach JE (1983) Paleoclimatic estimates from water and energy budgets of East African Lakes. *Quat Res* 19:141–153
- Hastenrath S, Kutzbach JE (1985) Late Pleistocene climate and water budget of the south American Altiplano. *Quat Res* 24:249–256
- Hu RJ, Yang CD, Ma H, Jiang FQ, Urkunbek (1994) Glaciers and lakes in the Tianshan Mountains and climate trends. *Arid Land Geogr* 17:1–7 (in Chinese with English abstract)
- Hu G, Wang NA, Zhao Q, Cheng HY, Chen YS, Guo JY (2003) Water balance of Huahai Lake Basin during a special phase. *J Gliciol Geocryol* 25:485–490 (in Chinese with English abstract)
- Jia YL, Shi YF, Fan YQ (2000) Water balance of paleolake Qinghai and its precipitation estimation at three high lake-level stages since 40 ka BP. *J Lake Sci* 12:211–218 (in Chinese with English abstract)
- Jia YL, Shi YF, Cao JT, Fan YC (2001a) The precipitation of the interior lakes in the southwestern Tibetan Plateau at 40~30 ka BP. *Adv Earth Sci* 16:346–351 (in Chinese with English abstract)
- Jia YL, Shi YF, Fan YQ (2001b) A method on determining the parameters of the hydrological and energy-balance model and its use: a case study of Qinghai Lake at Holocene megathermal. *Adv Water Sci* 12:324–330 (in Chinese with English abstract)
- Jia YL, Ma CM, Zhu C, Wei L, Wang PL (2004) Past, present and future of estimates of paleoprecipitation in closed lake basin. *Scientia Geographica Sinica* 24:376–383 (in Chinese with English abstract)
- Jia WX, He YQ, Wang XF, Li ZX (2009) Temporal and spatial change of the potential evaporation over Qilian mountains and Hexi corridor from 1960 to 2006. *Adv Water Sci* 20:159–167 (in Chinese with English abstract)
- Kou YG, Zeng JZ, Xie WR, Xiao S (1981) Investigation of radiation on Qinghai-Xizang Plateau and its neighbouring districts and the relation between radiation and permafrost on it. *J Gliciol Geocryol* 3:25–31 (in Chinese with English abstract)
- Kutzbach JE (1980) Estimates of past climate at Paleolake Chad, North Africa, based on a hydrological and energy-balance model. *Quat Res* 14:47–82
- Lan YC, Ding YJ, Kang ES (2004) Variations and trends of temperature and precipitation in the mountain drainage basin of the Heihe River in recent 50 years. *Plateau Meteorol* 23:723–727 (in Chinese with English abstract)
- Lan YC, Ding YJ, Liu JQ, Kang ES, Wei Z (2005) Change of water resources in mountainous area of Heihe River under global-warming scene. *J Desert Res* 25:863–868 (in Chinese with English abstract)
- Li DL, Liu HL (2004) Responding of Heihe river runoff to decadal climate change in Qilian mountain area. *J Desert Res* 24:385–391 (in Chinese with English abstract)
- Li Y, Morrill C (2010) Multiple factors causing Holocene lake-level change in monsoonal and arid central Asia as identified by model experiments. *Clim Dyn* 35:1119–1132
- Li S, Nu G, Li Y, Gong J (1999) Sustainable development and rational utilization of water resources in the Hexi Corridor Area. Environment Science Press, Beijing, pp 4–5, 14–36 (in Chinese)
- Li S, Li F, Sun W, Li BS (2004) Modern desertification process in Ejina Oasis and its dynamic mechanism. *Scientia Geographica Sinica* 24:61–67 (in Chinese with English abstract)
- Li CZ, Yu FL, Liu J (2009) Dynamic change of landscape and its driving forces in midstream of Heihe mainstream basin after water redistribution. *Acta Ecol Sinica* 29:5832–5842 (in Chinese with English abstract)
- Li XM, Lu L, Yang WF, Cheng GD (2012a) Estimation of evapotranspiration in an arid region by remote sensing—a case study in the middle reaches of the Heihe River Basin. *Int J Appl Earth Obs Geoinf* 17:85–93
- Li ZL, Wang NA, Li Y, Lai TT, Lu JW (2012b) Variations of runoff in responding to climate change in mountainous areas of Heihe River during last 50 years. *Bull Soil Water Conserv* 32(2):7–16 (in Chinese with English abstract)
- Liu Y, Sun JY, Song HM, Cai QF, Bao GA, Li XX (2010) Tree-ring hydrologic reconstructions for the Heihe River watershed, western China since AD 1430. *Water Res* 44:2781–2792
- Ma N, Wang NA, Li ZL, Chen XL, Zhu JF, Dong CY (2011) Analysis on climate change in the northern and southern marginal zones of the Badain Jaran Desert during the period 1960–2009. *Arid Zone Res* 28:242–250 (in Chinese with English abstract)
- Nie ZL, CHEN ZY, Cheng XX, Hao ML, Zhang GH (2005) The chemical information of the interaction of unconfined groundwater and surface water along the Heihe River, Northwestern China. *J Jilin Univ (Earth Sci Ed)* 35:48–53 (in Chinese with English abstract)
- Pederson N, Jacoby GC, D'Arrigo RD, Cook ER, Buckley BM, Dugarjav C, Mijiddorj R (2001) Hydrometeorological reconstructions for Northeastern Mongolia derived from tree rings: AD 1651–1995. *J Clim* 14:872–881
- Polacek D, Kofler W, Oberhuber W (2006) Radial growth of *Pinus sylvestris* growing on alluvial terraces is sensitive to water-level fluctuations. *New Phytol* 169:299–308
- Priestley CHB, Taylor RJ (1972) On the assessment of surface heat flux and evaporation using large-scale parameters. *Mon Weather Rev* 100:81–92
- Qian YP, Wang L (2008) Isotope hydrology used in the hydrologic cycle during the Heihe river basin. The Yellow River Water Conservancy Press, Zhengzhou, pp 1–10 (in Chinese)
- Qin BQ (1997) Estimates of paleo-hydrological parameters and water balance of Qinghai Lake with energy-water balance model. *Oceanologia Limnologia Sinica* 28:611–616 (in Chinese with English abstract)
- Qin C, Yang B, Burchardt I, Hu X, Kang XC (2010) Intensified pluvial conditions during the twentieth century in the inland Heihe River Basin in arid northwestern China over the past millennium. *Global Planet Change* 72:192–200
- Qin DJ, Qian YP, Han LF, Wang ZM, Li C, Zhao ZF (2011) Assessing impact of irrigation water on groundwater recharge and quality in arid environment using CFCs, tritium and stable isotopes, in the Zhangye Basin, Northwest China. *J Hydrol* 405:194–208
- Qu YG (1994) Water balance and forecasting of water level change in Qinghai Lake. *J Lake Sci* 6:298–307 (in Chinese with English abstract)
- Rhode D, Ma HZ, Madsen DB, Brantingham PJ, Forman SL, Olsen JW (2010) Paleoenvironmental and archaeological investigations at Qinghai Lake, western China: geomorphic and chronometric evidence of lake level history. *Quat Int* 218:29–44
- Schumm SA (1965) Quaternary paleohydrology. In: Wright HE, Frey DG (eds) *The quaternary of the United States*. Princeton University Press, Princeton, pp 783–794

- Schumm SA (1977) *The fluvial system*. John Wiley & Sons, New York, pp 27–48
- Sellers WD (1965) *Physical climatology*. University of Chicago Press, Chicago, pp 92–106
- Shen HY, Jia YL, Wei L (2005) Paleoprecipitation reconstruction during the interstadial of the Last Glacial (40–22 ka BP) in Huangqihai Lake, Inner Mongolia. *Acta Sedimentol Sin* 23:523–530 (in Chinese with English abstract)
- Shi YF (1990) Glacier recession and Lake Shrinkage indicating the climatic warming and drying trend in Central Asia. *Acta Geogr Sin* 45:1–11 (in Chinese with English abstract)
- Shi YF, Shen YP, Hu RJ (2002) Preliminary study on signal, impact and foreground of climatic shift from warm-dry to warm-humid in northwest China. *J Glaciol Geocryol* 24:219–224 (in Chinese with English abstract)
- Su CX, Hu YQ (1987) Oasis and lake Cold Island. *Chinese Sci Bull* 32:756–758 (in Chinese)
- Su YH, Feng Q, Zhu GF, Si JH, Zhang YW (2007) Identification and evolution of groundwater chemistry in the Ejin Sub-Basin of the Heihe River, Northwest China. *Pedosphere* 17:331–342
- Swain AM, Kutzbach JE, Hastenrath S (1983) Estimates of Holocene precipitation for Rajasthan, India, based on pollen and lake-level data. *Quat Res* 19:1–17
- Wang Z, Liu C, You G (1981) Glacier inventory of China I, Qilian Mountains, Lanzhou Institute of Glaciology and Geocryology, Academia Sinica, pp 59–119 (in Chinese)
- Wang SG, Dong GR, Li XL, Jin J (2000) Advances in studying sand-dust storms of China. *J Desert Res* 20:349–356 (in Chinese with English abstract)
- Wang HY, Shi CY, Wang MH, Xie Q, Hao JM, Li L (2004) Inferences of the past annual runoff of the early and middle Holocene for Quzhou area, the southern Hebei Plain. *Geogr Res* 23:183–191 (in Chinese with English abstract)
- Wang H, Hu ZY, Li DL, Zhao YZ, Ma WQ (2009) Comparative of climatologic characteristics of the surface radiation balance on Dingxin Gobi and Zhangye Oasis and desert underlying surfaces in Heihe Watershed, Gansu. *J Glaciol Geocryol* 31:464–473 (in Chinese with English abstract)
- Wang NA, Li ZL, Cheng HY, Li Yu, Huang YZ (2011) High lake levels on Alxa Plateau during the Late Quaternary. *Chinese Sci Bull* 56:1799–1808
- Winkler MG, Swain AM, Kutzbach JE (1986) Middle Holocene dry period in the northern Midwestern United States: Lake Levels and pollen stratigraphy. *Quat Res* 25:235–250
- Wu JL, Wang HD, Wang SM (1993) Paleoclimatic estimate during the last 10000 years in Ebinur Lake, Xinjiang. *J Lake Sci* 5:299–306 (in Chinese with English abstract)
- Wu Y, Wen X, Zhang Y (2004) Analysis of the exchange of groundwater and river water by using Radon-222 in the middle Heihe Basin of northwestern China. *Environ Geol* 45:647–653
- Wu JK, Ding Y, Ye B, Yang Q, Zhang X, Wang J (2010a) Spatio-temporal variation of stable isotopes in precipitation in the Heihe River Basin, Northwestern China. *Environ Earth Sci* 61:1123–1134
- Wu YQ, Zhang YH, Wen XH, Su JP (2010b) Hydrologic cycle and water resource modeling for the Heihe River Basin in Northwestern China. Science Press, Beijing, pp 98–190 (in Chinese)
- Yang Z (1991) *Glacier water resources in China*. Science Press, Beijing, pp 119–136 (in Chinese)
- Yu G, Xue B, Liu J, Chen X, Zheng YQ (2001) *Lake records from China and the palaeoclimate dynamics*. China Meteorological Press, Beijing, pp 1–94 (in Chinese)
- Zhang LJ, Zhao WZ (2008) Daily precipitation pattern and its temporal variability in Heihe River Basin. *J Desert Res* 28(4):741–747 (in Chinese with English abstract)
- Zhang HC, Peng JL, Ma YZ, Chen GJ, Feng ZD, Li B, Fan HF, Chang FQ, Lei GL, Wünnemann B (2004) Late Quaternary palaeolake levels in Tengger Desert, NW China. *Palaeogeogr Palaeoclimatol Palaeoecol* 211:45–58
- Zhang K, Wang RY, Han HT, Wang XP, Si JH (2007) Hydrological and water resources effects under Climate Change in Heihe River Basin. *Resour Sci* 29:77–83 (in Chinese with English abstract)
- Zhao WZ, Liu B (2010) The response of sap flow in shrubs to rainfall pulses in the desert region of China. *Agr Forest Meteorol* 150:1297–1306
- Zhao Q, Li XM, Wang NA (2007) Water balance of Shiyang River drainage During 6700–5800 yr BP. *J Arid Land Resour Environ* 21(6):84–91 (in Chinese with English abstract)
- Zhao WZ, Niu ZR, Chang XL, Li SB (2010) Water consumption in artificial desert oasis based on net primary productivity. *Sci China Earth Sci* 53:1358–1364
- Zhou J, Li X, Wang GX, Zhao J (2009) The spatio-temporal variation analysis of groundwater and response to land-use change in the Middle Reaches of the Heihe River Basin. *J Nat Resour* 24:498–506 (in Chinese with English abstract)
- Zhu YH, Wu YQ, Drake S (2004) A survey: obstacles and strategies for the development of ground-water resources in arid inland river basins of Western China. *J Arid Environ* 59:351–367
- Zhu LP, Xie MP, Wu YH (2010) Quantitative analysis of lake area variations and the influence factors from 1971 to 2004 in the Nam Co basin of the Tibetan Plateau. *Chinese Sci Bull* 55:1294–1303
- Zuo HC, Lv SH, Hu YQ, Ma YM (2004) Observation and numerical simulation of heterogenous underlying surface boundary layer (I): the whole physical picture of Cold Island effect and inverse humidity. *Plateau Meteorol* 23:155–162 (in Chinese with English abstract)